A single shear band in a metallic glass: Local core and wide soft zone

R. Maaß, K. Samwer, W. Arnold, and C. A. Volkert

Citation: Applied Physics Letters **105**, 171902 (2014); doi: 10.1063/1.4900791
View online: http://dx.doi.org/10.1063/1.4900791
View Table of Contents: http://scitation.aip.org/content/aip/journal/apl/105/17?ver=pdfcov
Published by the AIP Publishing

A single shear band in a metallic glass: Local core and wide soft zone

R. Maaß,[1,a)] K. Samwer,[2] W. Arnold,[2,3] and C. A. Volkert[1]
[1]*Institute for Materials Physics, University of Göttingen, Friedrich-Hund Platz 1, 37077 Göttingen, Germany*
[2]*1st Physics Institute, University of Göttingen, Friedrich-Hund Platz 1, 37077 Göttingen, Germany*
[3]*Department of Materials and Materials Technology, Saarland University, Campus D2.2, 66123 Saarbrücken, Germany*

(Received 22 September 2014; accepted 19 October 2014; published online 29 October 2014)

Two dimensional mapping of structural properties near a single shear band in a Zr-based bulk metallic glass reveals the presence of hardness and modulus reductions at a micrometer length scale. The isolated shear band had carried all the macroscopic plastic strain and the material near the shear-band exhibits structural variations both along and normal to the shear plane. Analyzing the nanoindentation data indicates that long range internal stresses are the primary cause of the spatially varying structure. The results demonstrate that a nano-scale defect in a metallic glass may have a micrometer range signature. © *2014 AIP Publishing LLC*.
[http://dx.doi.org/10.1063/1.4900791]

Metals with a disordered atomic structure, that is metallic glasses (MGs), are a special class of materials with extraordinary physical and mechanical properties.[1] With production routes that allow bulk casting as well as rapid thermoplastic forming, major steps towards structural applications have been taken.[2,3] Despite many advantages compared to conventional structural crystalline materials, MGs lack intrinsic strain hardening and have a tendency to fail rapidly upon the formation of planar, localized defects, called shear bands. Such defects are both good and bad; good because they allow the dissipation of energy and conversion to plastic strain, and bad because they are hard to control and they are promoting structural failure. Thus, there is great scientific interest in understanding shear bands in MGs, with the aim of finding tuneable parameters that eventually will allow predictable and controllable levels of stable plastic flow.

The characterization of shear bands remains an experimental challenge, because their spatial extent normal to the shear plane is said to be in the nm-regime,[4] with selected evidence for a thickness increase as a function of plastic strain.[5] Furthermore, shear-band operations are occurring on the ms time scale at room temperature,[6,7] which makes *in-situ* measurements a delicate task. Since shear-band dynamics has been shown to be thermally activated, low temperature experiments allow to substantially increase the active shear-banding time by up to a factor of 1000.[7] In fact, low temperature measurements of shear-band dynamics gave direct insights into both static shear-band aging and shear-band creep, evidencing structural dynamics of the shear-band material during its active phase.[8] However, such studies are scarce, and further efforts to characterize shear-band structure *in-situ* are required. Consequently, most investigations concentrate on post-mortem studies of formed, but inactive shear bands.

Since shear bands are believed to have thickness of few nanometers, nanoindentation is a suitable technique to probe the structural signature in the vicinity of shear bands on the surface of a MG. This approach has been followed by numerous authors,[9–11] with the caveat that the analysed material contained a dense shear-band structure with a shear-band spacing that is much smaller or of the same length scale as the used indentation probe. The dense shear-band structure is a direct signature of a non-trivial three dimensional stress state during plastic straining,[12,13] and is hard to control. In addition, a mapping of nanoscale structural parameters across a region of densely spaced shear bands blurs the obtained data due to height offsets that contribute with a non negligible topological error. Ideally, nanoscale structural probing is performed near a single shear band.

In this letter, we are able to isolate a single shear band from a Zr-based bulk MG. Along this one shear band, which had carried all plastic strain, we spatially resolve the structural changes normal to the shear band by nanoindentation. It is found that the indentation hardness profiles exhibit structural softening in the range of 5%–20%, depending on location along the shear band. Even though the shear-band plane is expected to be some nm thick, the softened profiles have a width exceeding tens of micrometers. The results are discussed in terms of changes in the atomic structure, as well as in terms of a residual stress state.

The investigated material ($Zr_{52.2}Ti_5Cu_{17.9}Ni_{14.6}Al_{10}$, Vit105) was produced with an arc melter by conventional suction casting into a Cu mold. Compression samples with a 3 mm diameter were strained in the non-serrated flow regime with a constant applied strain rate of 10^{-3} s^{-1} at −100 °C. Similarly, as in Refs. 13 and 14, the samples were notched to introduce a defined location for shear-band initiation, which allows unconstrained shear-band propagation of a single shear band. The samples were unloaded prior to failure, placed on a substrate and polished to obtain a cross-sectional flat surface on which the shear-band line could be traced with the help of the shear-offsets. The final polishing stages comprised of a 40 nm Al_2O_3 suspension, followed by lubricated polishing on a clean disc, free of any polishing particles. The obtained surface was analyzed with AFM (Asylum MFP-3D) in non-contact mode, yielding a root mean square roughness of 4.9 nm over an area of

a)Electronic mail: robert.maass@ingenieur.de

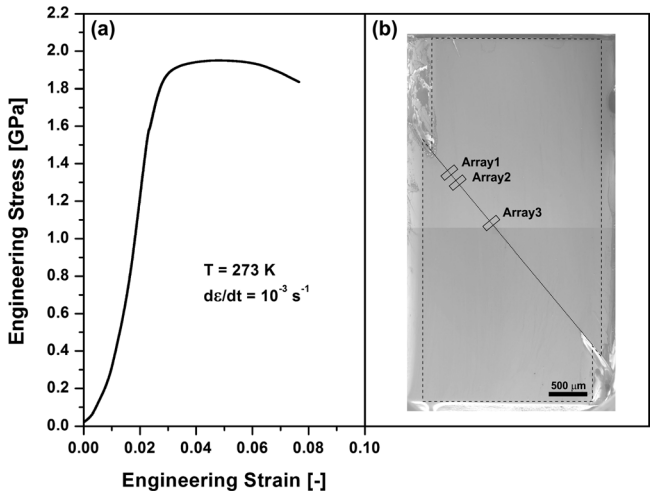

FIG. 1. (a) Non-serrated flow curve of a $Zr_{52.2}Ti_5Cu_{17.9}Ni_{14.6}Al_{10}$ recorded at 273 K. (b) Cross-sectional SEM view, where the line indicates the location (not to scale) of the shear-band, and three sites of nanoindentation mapping are shown. The dashed line marks the approximate border of the polished area.

$20 \times 20\,\mu m2$. Nanoindentation was conducted with an Agilent G200 device, using the dynamic contact module (DCM) low load indentation head and a conical diamond tip with a radius of 650 nm. This large tip was intentionally chosen to avoid influences from surface roughness and to sample large volumes. All indents were done in load control at a rate of 0.25 mN/s to a maximum load of 5 mN, with an indent spacing of 3 to 6 μm, probing a depth of ~240 nm in the MG.

Figure 1(a) displays a stress-strain curve and Fig. 1(b) shows the corresponding scanning electron microscopy (SEM) micrograph of the polished surface. A solid line indicates the location of the shear-band line. Three sites, at which indentation arrays were measured, are indicated (not to scale). In the following, we will focus on the results of these three arrays.

The distance along the shear-band line between the three nanoindentation arrays was ~180 μm (1–2), and ~950 μm (2–3). Array 1 consisted of 200 indents, array 2 of 175 indents, and array 3 of 119 indents. Figure 2(a) shows exemplarily the change in indentation hardness, H, relative to the matrix value H_0 (average of 100 measurements far away from the shear-band line with a mean of 7.79 ± 0.17 GPa) for array 2. A clear drop in H is visible when probing across the location of the shear-band line. In fact, the softened region extends over a few tens of microns, and reaches a hardness decrease relative to the surrounding matrix of approximately 20%. The same trend, but much less pronounced, applies to the measured indentation modulus, $(E/E_0)\times 100$. It is also noted that there is not a 1:1 correlation between locations of strongly reduced H and E. For example, at location ($y = 15\,\mu m$; $x = 30\,\mu m$) H has dropped by ~20%, whereas E has only decreased marginally within the scatter (standard deviation = 1.8%) of the E-values. Although there is considerable scatter in the modulus map in Fig. 2(b), the same spatial correlation as for the hardness map emerges. Given the established values on shear-band thickness, the results in Fig. 2 are truly remarkable because they reveal a spatial signature that is ca. 3 orders of magnitude larger than the shear-band itself.

To further quantify the outcome depicted in Fig. 2, both the indentation hardness and the indentation modulus were averaged along the shear-band direction for all three sites, as shown in Fig. 1(b). The resulting averaged H- and E-profiles are summarized in Figure 3. Depending on array location along the shear-band line, different degrees of structural softening are seen (Fig. 3(a)): array 1 has a maximum mean hardness decrease of only 5%, array 2 shows 17.5%, and array 3 exhibits a maximum decrease of 10%. This is clear evidence for that the structural changes along the shear-band line are position dependent and that a direct correlation with macroscopic plastic strain cannot be established. At the nm-scale (size-regime of the shear-band thickness), position dependent local properties have been demonstrated with both acoustic AFM measurements, where intrinsic nano-scale fluctuations in elastic modulus are found in the as-cast state,[15] and also with transmission electron microscopy that revealed density fluctuations along a shear band.[16] Yet another earlier work, based on a single indentation row across a shear-band line, found comparable values of ΔH, but also a direct dependence between total plastic strain and softening.[5] The increase in the width of the softened region with increasing macroscopic strain was rationalized based on

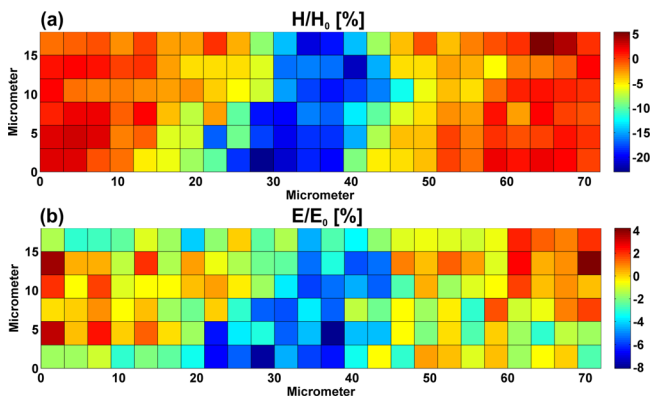

FIG. 2. Relative change of the indentation hardness (a) and modulus (b) across the shear-band line of array 2. Micrometer scale modulations are revealed along the nm-thick planar defect.

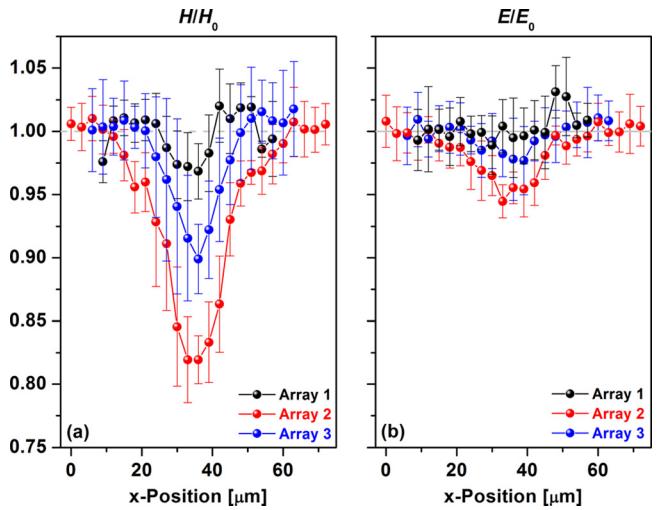

FIG. 3. Averaged profiles of both indentation hardness (a) and indentation modulus (b) obtained from the three arrays depicted in the inset in Fig. 1. Identical axis scaling applies to both graphs.

free volume accumulation and diffusion away from the shear-band core with a saturation value of ca. 2%, corresponding to $\Delta H_{max} = 36\%$. In a picture of diffusive shear with a free volume profile directly correlated to the softening profile, the present findings would indicate spatial variations along the shear-band line, without any distinct dependence on macroscopic plastic shear-strain at the local scale.

The data in Fig. 3(a) were fit to a Gaussian model, yielding the peak widths of the softened zone in terms of a full width at half maximum (FWHM). The larger the amount of structural softening, the wider is also the affected zone, reaching a FWHM of $20.6 \pm 0.8\,\mu$m in array 2; $14.4 \pm 0.7\,\mu$m in array 3; and $10.2 \pm 2.2\,\mu$m in array 1. In addition to ΔH, Fig. 3(b) also shows the corresponding ΔE-profiles for all three indentation arrays. Despite a higher degree of scatter as well as overall smaller magnitudes, there seems to be a correlation between ΔH and ΔE for arrays 2 and 3: the larger ΔH, the larger also ΔE. Whilst a local softening can be rationalized with existing theories on plasticity of MGs, a *long range* change in elastic properties of the order of 5%–6% is less straightforward. In fact, such high values have been reported for MGs under a hydrostatic pressure of 2 GPa, where the Young modulus (directly related to the indentation modulus) of MGs increases with about 5%–7%.[1] As such, it is concluded that the data in Fig. 3(b) suggest either strong internal stresses at the limit of the yield strength of the material or any potential structural changes during shear banding that occur via diffusion processes (at room temperature or 273 K) have a much larger spatial extent than can expected from bulk diffusion coefficients.

To further investigate the origin of the trends depicted in Figs. 2 and 3, the indentation imprint area, A, is imaged directly with SEM and subsequently evaluated using a custom designed image recognition code built with Matlab. This was done since it is known that residual tensile stresses can lead to an artificial reduction of both H and E via an incorrectly determined A during automated indentation.[17] This is clear when considering $H = P_{\max}/A$, with $P_{\max}$ being the maximum load, and the effective modulus $E_{eff} = (S\sqrt{\pi})/(2\beta\sqrt{A}) = f(E)$, where $\beta = 1$ for a spherical indenter and S is the contact stiffness at $P_{\max}$. As such, it is required to compare the imprint area derived by the indenter, A_{ind}, with the one directly determined with electron microscopy, A_{SEM}. This is done for both the matrix material as well as the apparently softened shear-band region. Figure 4 shows that the A_{ind} consistently exceeds A_{SEM}, which holds true for both matrix and shear-band material.

The reason for $A_{\text{ind}} > A_{\text{SEM}}$ is primarily thought to be caused by difficulties in exactly determining the border between imprint and matrix when calculating A_{SEM}, but it cannot be excluded that a minor contribution is due to residual surface stresses introduced by the polishing method. Due to the high ratio between surface roughness and indentation depth, we believe that this effect can be neglected. We further note that the spread in A_{SEM} is twice as large as for A_{ind} over the matrix material, but of similar width for the shear-band region. More important, however, is that both A_{ind} and A_{SEM} are consistently larger for the shear-band region, which indicates that the softening and the modulus reduction cannot primarily be ascribed to an error in the determination of A. An additional evidence for this conclusion is that the ratio $A_{\text{ind}}/A_{\text{SEM}}$ is identical for all values irrespective of matrix or shear-band material. That means, the effect seen in Figs. 3 and 4 can be taken as real, and is therefore in direct agreement with earlier work that linked a decrease in H to residual tensile stresses of an elastically strained MG.[18,19]

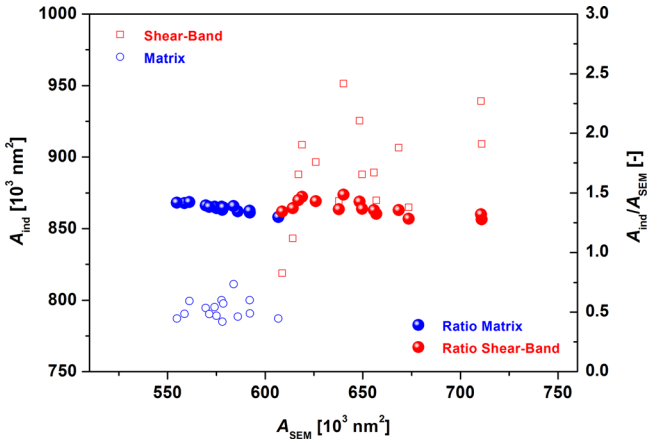

FIG. 4. Indentation imprint area derived by the nanoindenter as a function of the area directly measured with SEM for both the matrix and the shear-band material. The right y-axis also shows the ratio $A_{\text{ind}}/A_{\text{SEM}}$. Identical axis scaling is used for A_{ind} and A_{SEM}.

With these results at hand, we conclude that significant reductions in both H and E extending up to tens of microns can form near a shear band in a bulk metallic glass. There seem to be large variations along the shear-band, and the variation in E suggests internal stresses that are close to the yield stress of the material itself.[1] Since a shear band is not a perfectly flat shear plane with a certain degree of waviness, it is understood that inhomogeneously distributed stress fields develop along the shear plane during shear. Upon removal of the applied load, those are frozen in during shear-band arrest and can be revealed as seen in Fig. 2. This is very much in agreement with both tensile- and shear-deformation experiments that have revealed the introduction of internal stresses, whose magnitude is dependent on the initially applied shear stress.[20,21] A forthcoming study is underway to quantitatively support this interpretation.

Earlier indentation measurements that were conducted on a dense shear-band structure are thus expected to sensitively depend on the number of shear bands probed, and overlapping stress fields near several shear bands are therefore expected to yield an apparent trend with shear-band density. Interpretations based on shear-induced local structural dilatation (density decrease) have to be carefully examined with respect to present internal stress fields that we here conclude to accompany a single shear band. Finally, the present data demonstrate the difficulty in ascribing a shear-band one single length scale. Whilst the shear-band thickness may actually be of the order of some tens of nanometers, our results clearly show that this defect with a nano-scale core may have a long range signature at a length scale several orders of magnitude larger.

We are pleased to acknowledge experimental support by D. Tönnies and P. Birckigt. R.M. thanks the Laboratory for

Metals Physics and Technology at ETH Zurich (J. F. Löffler), where the samples where produced and macroscopically compressed as part of a different research project.

[1]W. H. Wang, C. Dong, and C. H. Shek, Mater. Sci. Eng., R **44**, 45–89 (2004).
[2]W. L. Johnson, G. Kaltenboeck, M. D. Demetriou, J. P. Schramm, X. Liu, K. Samwer, C. P. Kim, and D. C. Hofmann, Science **332**, 828–833 (2011).
[3]G. Kumar, A. Desai, and J. Schroers, Adv. Mater. **23**, 461–476 (2011).
[4]Y. Zhang and A. L. Greer, Appl. Phys. Lett. **89**, 071907 (2006).
[5]J. Pan, Q. Chen, L. Liu, and Y. Li, Acta Mater. **59**, 5146–5158 (2011).
[6]W. J. Wright, R. B. Schwarz, and W. D. Nix, Mater. Sci. Eng., A **319**, 229–232 (2001).
[7]R. Maass, D. Klaumuenzer, and J. F. Löffler, Acta Mater. **59**, 3205–3213 (2011).
[8]R. Maass, D. Klaumunzer, G. Villard, P. M. Derlet, and J. F. Loffler, Appl. Phys. Lett. **100**, 071904 (2012).
[9]B.-G. Yoo, Y.-J. Kim, J.-H. Oh, U. Ramamurty, and J.-I. Jang, Scr. Mater. **61**, 951–954 (2009).
[10]R. Bhowmick, R. Raghavan, K. Chattopadhyay, and U. Ramamurty, Acta Mater. **54**, 4221–4228 (2006).
[11]H. Bei, S. Xie, and E. P. George, Phys. Rev. Lett. **96**, 105503 (2006).
[12]W. F. Wu, Y. Li, and C. A. Schuh, Philos. Mag. **88**, 71–89 (2008).
[13]R. Maass, D. Klaumuenzer, E. I. Preiss, P. M. Derlet, and J. F. Löffler, Scr. Mater. **66**, 231–234 (2012).
[14]P. Thurnheer, R. Maass, S. Pogatscher, and J. F. Loffler, Appl. Phys. Lett. **104**, 101910 (2014).
[15]H. Wagner, D. Bedorf, S. Kuechemann, M. Schwabe, B. Zhang, W. Arnold, and K. Samwer, Nat. Mater. **10**, 439–442 (2011).
[16]H. Rösner, M. Peterlechner, C. Kuebel, V. Schmidt, and G. Wilde, Ultramicroscopy **142**, 1–9 (2014).
[17]T. Y. Tsui, W. C. Oliver, and G. M. Pharr, J. Mater. Res. **11**, 752–759 (1996).
[18]L. Y. Chen, Q. Ge, S. Qu, and J. Z. Jiang, Scr. Mater. **59**, 1210–1213 (2008).
[19]L. Wang, H. Bei, Y. F. Gao, Z. P. Lu, and T. G. Nieh, Acta Mater. **59**, 7627–7633 (2011).
[20]V. A. Khonik and T. N. Ryabtseva, Scr. Metall. Mater. **30**, 571–575 (1994).
[21]G. V. Afonin, S. V. Khonik, R. A. Konchakov, N. P. Kobelev, A. A. Kaloyan, and V. A. Khonik, J. Non-Cryst. Solids **358**, 220–223 (2012).